A Non-centrosymmetric Chalcohalide Synthesized through Combination of Chemical Tailoring with Aliovalent Substitution

Yufei Song,[a] Zhen Qian,[a] Boru Zhou,[a] Hongwei Yu,[a] Zhanggui Hu,[a] Jiyang Wang[a], Yicheng Wu[a], and Hongping Wu,[a*]

Tianjin Key Laboratory of Functional Crystal Materials, Institute of Functional Crystal, Tianjin University of Technology, Tianjin 300384, China.

To whom correspondence should be addressed. E-mail: wuhp@ms.xjb.ac.cn (Hongping Wu).

CONTENTS

Experimental Section

Materials. LiCl (99.5%), $SrCl_2$ (99.5%), SrS (99.99%), Ge (99.99%) and S (99.9%) were purchased from Fuchen (Tianjin) Chemical Reagent Co. Ltd, Shanghai Aladdin Biochemical Technology Co. Ltd, and Beijing Hawk Science and Technology Co. Ltd. (China), respectively.

Synthesis. All the starting materials were used as purchased and stored in a glovebox filled with purified Ar (moisture and oxygen level is less than 0.1 ppm), and all manipulations were performed inside the glovebox. The crystal of $[Sr_4Cl_2][Ge_3S_9]$ was prepared with a mixture of SrS, Ge, and S (1:1:3 molar ratio), and an appropriate amount of flux with a total mass of 0.105g LiCl and 0.395g $SrCl_2$. Then the mixture was loaded into fused silica tube under a vacuum of 10^{-3} Pa. Next, the fused silica tube was put in the furnace and annealed at 1223 K for 50 h and then kept at this temperature for 100 h to ensure the mixture completely melted. This was followed by slowly cooling at 3 K/h to 473 K, and then the furnace was turned off. The anhydrous ethanol and N, N-dimethylformamide (DMF) were used to wash the reaction products for removing the other byproducts. Finally, the crystal was obtained, which was stable in the air for several months.

Polycrystalline sample of $[Sr_4Cl_2][Ge_3S_9]$ could be easily synthesized by heating stoichiometric mixtures sealed into an evacuated silica tube at 1123 K for 2 days. The purity of sample has been confirmed by the powder X-ray diffraction (PXRD).

Structure Determination. Single crystal XRD data was collected on a Bruker SMART APEX II CCD single crystal diffractometer at room temperature with Mo *Kα* radiation (λ = 0.71073 Å). The collected data was integrated by the SAINT program.[1] The data was analyzed and refined using the SHELXS program to obtain the final crystal structure data.[2, 3] The final structure was checked with PLATON,[4] and no other higher symmetry elements were found. The crystallographic data and structure refinement parameters are presented in Table 1. The atomic coordinates, equivalent isotropic atomic displacement parameters, the bond valence calculations for all atoms, and the selected distances (Å) and angles (deg.) are summarized in Table S2 and S3.

Powder X-ray Diffraction. PXRD data was collected using a SmartLab 9KW X-ray diffractometer at room temperature (Cu *Kα* radiation) with the scanning ranges of 10−70° in 2θ and a scan step of 2° min^{-1}. The measurement result shows that the PXRD pattern of the as-synthesized sample matches with the calculated one derived from the single crystal data (Fig. S1).

Energy-Dispersive Spectroscopy (EDS). Microprobe elemental analysis and the elemental distribution maps were measured on a field-emission scanning electron microscope (Quanta FEG 250) made by FEI. The EDS experiment indicates that the average atomic ratio of Sr, Ge, S, Cl is 22.22% : 16.67% : 50.00% : 11.11% for $[Sr_4Cl_2][Ge_3S_9]$, which is approximately equal to the theoretical ones (Fig. S2).

UV−Vis−Near-IR (NIR) Diffuse Reflectance Spectrum. The UV-Vis-NIR diffuse reflectance spectrum was measured in the range of 200−2000 nm using a Shimadzu SolidSpec-3700DUV Spectrophotometer at room temperature. $BaSO_4$ was utilized as the standard. Absorption (K/S) data was also calculated from the following Kubelka–Munk function: $F(R) = (1-R)^2/2R = K/S$, R represents the reflectance, K the absorption, and S the scattering factor.[5]

IR Spectrum. The IR spectrum of $[Sr_4Cl_2][Ge_3S_9]$ was recorded by a Nicolet iS50 FT-IR spectrometer with ATR in the range of 2.5−25 μm at room temperature. About 5 mg polycrystalline sample was placed on the test platform for testing.

Raman Spectrum. The Raman spectrum on the crushed crystal of $[Sr_4Cl_2][Ge_3S_9]$ was collected by a LABRAM HR Evolution spectrometer equipped with a CCD detector using 532 nm radiations from a diode laser. The sample was placed on a glass slide and a 50 × objective lens was used to choose the area of the crystal specimen to be measured. The maximum power of 60 mW and beam diameter of 35 μm was used. The spectrum was collected using an integration time of 5 s.

Power SHG Measurement. The powder SHG measurement was carried out with irradiation of a 2090 nm laser by using the modified Kurtz-Perry method to evaluate the frequency conversion ability of $[Sr_4Cl_2][Ge_3S_9]$.[6] The sample was ground and sieved in the range of 54−100, 100−125, 125−150, 150−180, and 180−225 μm, respectively. And a powder AGS sample with the same particle size range was used as a reference.

The Details of Computational Methods. On the basis of density functional theory (DFT),[7] the electronic band structure, the partial density of states, and optical properties for $[Sr_4Cl_2][Ge_3S_9]$ were implemented in the CASTEP package. In order to describe the exchange-correlation energy, we used a Perdew-Burke-Ernzerhof (PBE)[8] functional in the generalized gradient approximation (GGA).[9] The optimized norm-conserving pseudopotentials in the Kleinman-Bylander form were used to model the effective interactions between valence electrons and the atom cores. Sr $4S^24p^65s^2$, Ge $4s^24p^2$, S $3s^23p^4$, Cl $3s^23p^5$ electrons were set to be the valence electrons. The plane-wave energy cut-off value was set at 810.0 eV and the *k*-point grid sampling in the Monkhorst Pack scheme was set at 4 × 4 × 4 in the Brillouin zone. On the basis of the electron transition from the valence band (VB) to the conduction band (CB), we deduced the imaginary part of the dielectric function. Then, by using the Kramers-Kronig transform, we calculated the real part of the dielectric function.[10] The refractive indices n (and the birefringence Δn) were obtained from the real part of the dielectric function.

Table S1. Crystal data for $[Sr_4Cl_2][Ge_3S_9]$.

Empirical formula	$Sr_4Cl_2Ge_3S_9$
Formula weight	927.69
Temperature (K)	273(2)
Crystal system	Hexagonal
Space group	$P6_3$
a (Å)	9.519(3)
c (Å)	11.726(8)
Volume(Å^3)	920.2 (9)
Z	2
D_c (g cm^{-3})	3.348
μ (mm^{-1})	17.622
F(000)	852
2θ range (º)	2.47 to 27.47
Completeness to theta	100%
GOF on F^2	1.040
R_1, wR_2 (I >2σ(I))[a]	0.0473, 0.0830
R_1, wR_2 (all data)	0.0862, 0.0951
Flack x parameter	0.246 (0.023)
Largest diff. peak and hole(eÅ^{-3})	0.825 and -0.900

[a] $R_1 = \sum||F_o| - |F_c||/\sum|F_o|$, $wR_2 = \{\sum w[(F_o^2 - F_c^2)^2]/\sum w[(F_o^2)^2]\}^{1/2}$ for $F_o^2 > 2\sigma(F_o^2)$

Table S2. Atomic coordinates and equivalent isotropic atomic displacement parameters ($Å^2$), bond valence sums (BVSs) for $[Sr_4Cl_2][Ge_3S_9]$.

$Sr_4Cl_2Ge_3S_9$

Atom	x/a	y/b	z/c	U(eq)	BVS
Sr1	0.666667	0.333333	0.4410(2)	0.0190(6)	2.32
Sr2	0.3319(2)	0.2479(2)	0.12034(18)	0.0364(5)	1.78
Ge1	0.44607(17)	0.33498(18)	0.78445(12)	0.0167(4)	4.22
S1	0.4426(5)	0.1110(5)	0.8469(4)	0.0244(10)	2.08
S2	0.2456(5)	0.3215(5)	0.8805(4)	0.0241(10)	1.91
S3	0.4245(5)	0.3477(6)	0.6023(4)	0.0289(11)	1.92
Cl1	0.666667	0.333333	0.1803(7)	0.0273(18)	0.95
Cl2	0	0	0.1398(10)	0.052(3)	0.94

Table S3. Selected bond distances (Å) and angles (°) for for $[Sr_4Cl_2][Ge_3S_9]$.

$Sr_4Cl_2Ge_3S_9$

Atom–Atom	**Length [Å]**	S3#6-Sr1-S3	85.31(13)
Sr1-S3#3	3.038(4)	S3#4-Sr1-S3	85.31(13)
Sr1-S3	3.038(4)	S3#4-Sr1-S2#13	69.08(11)
Sr1-S2#7	3.042(4)	S3#6-Sr1-S2#10	153.03(14)
Sr1-Cl1	3.057(8)	S3-Sr1-S2#10	69.08(11)
Ge1-S3	2.155(4)	S3#6-Sr1-S2#7	69.08(11)
Ge1-S1	2.239(4)	S3-Sr1-S2#7	84.34(12)
Sr2-Cl2	2.854(19)	S2#10-Sr1-S2#7	114.74(7)
Sr2-S2#1	3.106(5)	S3#4-Sr1-Cl1	128.52(9)
Sr2-S1#8	3.240(5)	S3#6-Sr1-S2#13	84.34(12)
Sr2-S2#7	3.440(5)	S3-Sr1-S2#13	153.03(14)
Sr1-S3#2	3.038(4)	S3#4-Sr1-S2#10	84.34(12)
Sr1-S2#9	3.042(4)	S2#13-Sr1-S2#10	114.74(8)
Sr1-S2#4	3.042(4)	S3#4-Sr1-S2#7	153.03(14)
Ge1-S2	2.164(4)	S2#13-Sr1-S2#7	114.74(8)
Ge1-S1#3	2.240(5)	S3#6-Sr1-Cl1	128.52(9)
Sr2-Cl1	2.953(3)	S3-Sr1-Cl1	128.52(9)
Sr2-S3#7	3.176(4)	S2#10-Sr1-Cl1	76.52(10)
Sr2-S3#4	3.364(5)	S3-Ge1-S1	114.91(17)
Sr2-S3#8	3.584(5)	S3-Ge1-S1#6	110.03(17)
Atom–Atom–Atom	**Angle [°]**	S1-Ge1-S1#6	110.5(2)
S2#13-Sr1-Cl1	76.52(10)	Cl2-Sr2-S2#1	87.2(2)
S2#7-Sr1-Cl1	76.52(10)	Cl2-Sr2-S3#10	76.83(10)
S3-Ge1-S2	114.40(18)	S2#1-Sr2-S3#10	107.81(12)
S2-Ge1-S1	100.40(17)	Cl1-Sr2-S1#12	87.52(15)
S2-Ge1-S1#6	105.93(16)	S3#10-Sr2-S1#12	128.70(13)
Cl2-Sr2-Cl1	143.57(15)	Cl1-Sr2-S3#7	70.62(8)
Cl1-Sr2-S2#1	121.61(17)	S3#10-Sr2-S3#7	140.22(14)
Cl1-Sr2-S3#10	73.39(9)	Cl2-Sr2-S2#10	77.2(2)
Cl2-Sr2-S1#12	95.2(2)	S2#1-Sr2-S2#10	164.20(14)
S2#1-Sr2-S1#12	122.50(11)	S1#12-Sr2-S2#10	62.42(11)
Cl2-Sr2-S3#7	142.76(9)	Cl2-Sr2-S3#12	70.32(7)
S2#1-Sr2-S3#7	78.10(12)	S2#1-Sr2-S3#12	61.53(11)
S1#12-Sr2-S3#7	66.06(11)	S1#12-Sr2-S3#12	65.51(10)
Cl1-Sr2-S2#10	71.95(15)	S2#10-Sr2-S3#12	114.23(11)

S3#10-Sr2-S2#10	66.42(11)	S3#7-Sr2-S3#12	72.59(13)
S3#7-Sr2-S2#10	116.08(11)	S3#10-Sr2-S3#12	145.63(12)
Cl1-Sr2-S3#12	140.87(9)		

Symmetry transformations used to generate equivalent atoms:

#1	x, y, z-1	#2	x, y, z+1	#3	-y, x-y, z	#4	-y+1, x-y, z
#5	-x+y, -x, z	#6	-x+y+1, -x+1, z	#7	-x+1, -y+1, z-1/2	#8	-x+1, -y+1, z+1/2
#9	y, -x+y, z+1/2	#10	y, -x+y, z-1/2	#11	x-y, x, z+1/2	#12	x-y, x, z-1/2
#13	x-y+1, x, z-1/2	#14	x-y+1, x, z+1/2				

Table S4. The magnitude of Dipole Moments of $[NaSr_4Cl][Ge_3S_{10}]$ and $[Sr_4Cl_2][Ge_3S_9]$.

Crystals	anionic group	*x(a)*	*y(b)*	*z (c)*	Dipole Moment (D)	Dipole Moment ($\times 10^{-2}$ esu·cm^2/Å^3)
$NaSr_4ClGe_3S_{10}$	Ge_3S_9	0	0	-12.43	12.43	2.66
$Sr_4Cl_2Ge_3S_9$	Ge_3S_9	0	0	11.81	11.81	2.57

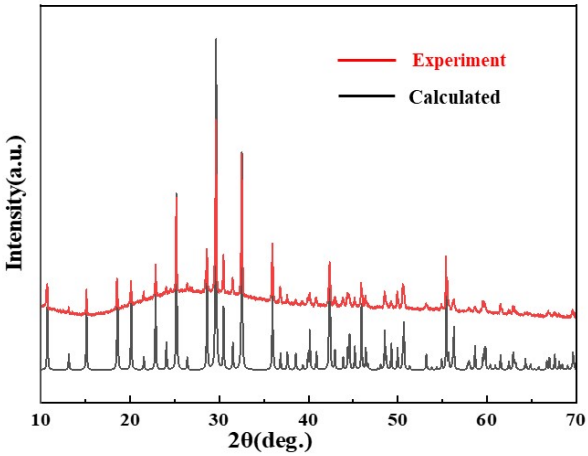

Fig. S1. Powder-XRD patterns of $[Sr_4Cl_2][Ge_3S_9]$.

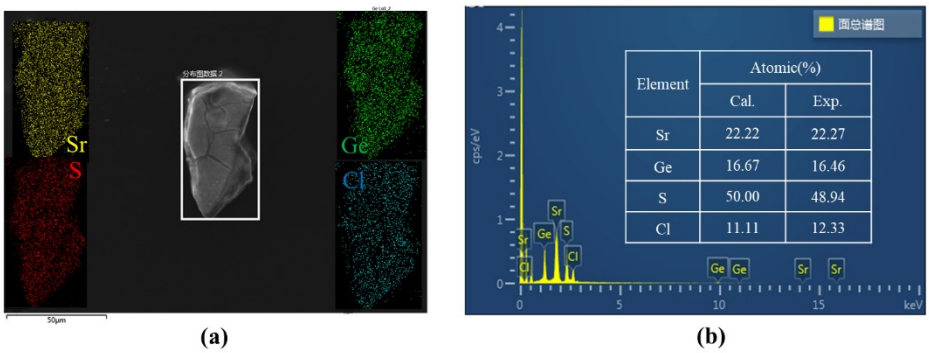

Element	Atomic(%)	
	Cal.	Exp.
Sr	22.22	22.27
Ge	16.67	16.46
S	50.00	48.94
Cl	11.11	12.33

(a) **(b)**

Fig. S2. The EDS of $[Sr_4Cl_2][Ge_3S_9]$.

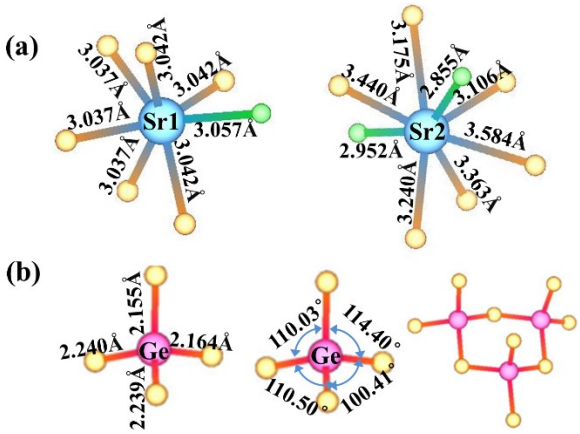

Fig. S3. The complete coordination environment of cations in $[Sr_4Cl_2][Ge_3S_9]$.

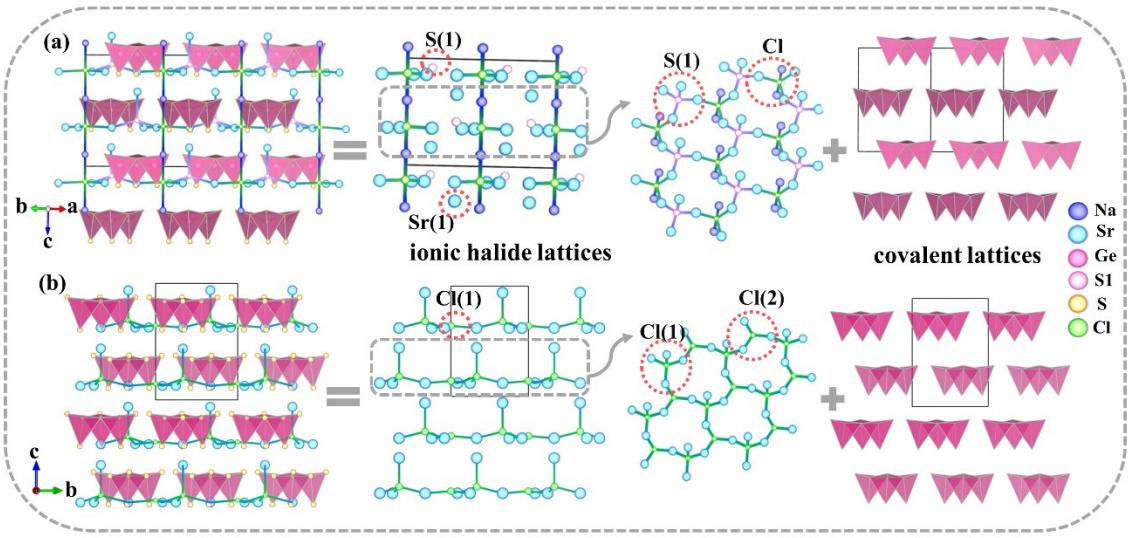

Fig. S4 Different structural configurations of ionic halide lattices and covalent sulfide lattices in the salt-inclusion chalcogenides of $[NaSr_4Cl][Ge_3S_{10}]$ (a), and $[Sr_4Cl_2][Ge_3S_9]$ (b).

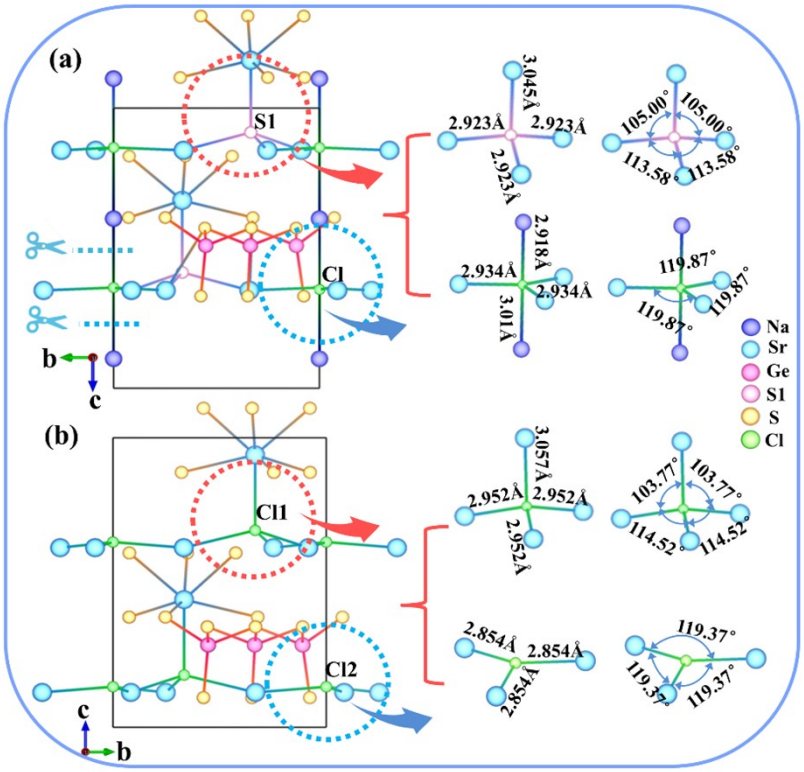

Fig. S5 The comparison of coordination environment of anions in $[NaSr_4Cl][Ge_3S_{10}]$ (a), and $[Sr_4Cl_2][Ge_3S_9]$ (b).

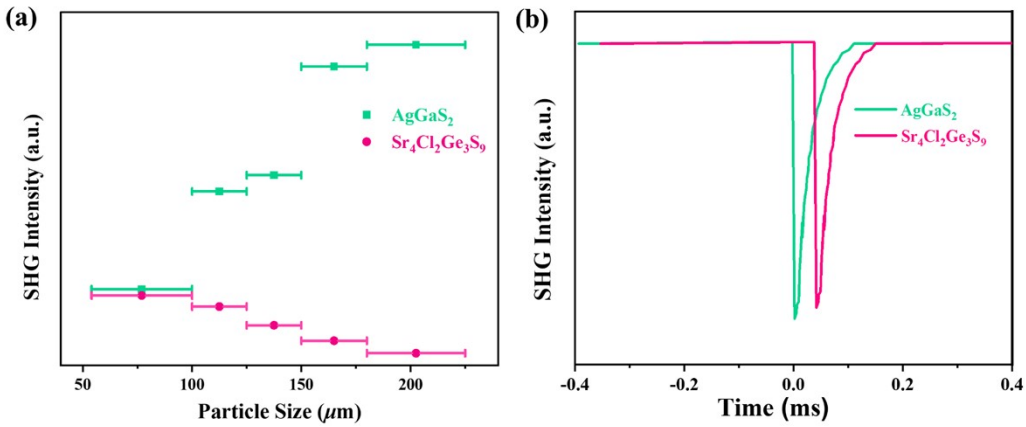

Fig. S6 The SHG intensities of $[Sr_4Cl_2][Ge_3S_9]$ (a), and $AgGaS_2$ at a particle size of 54−100 μm (b).

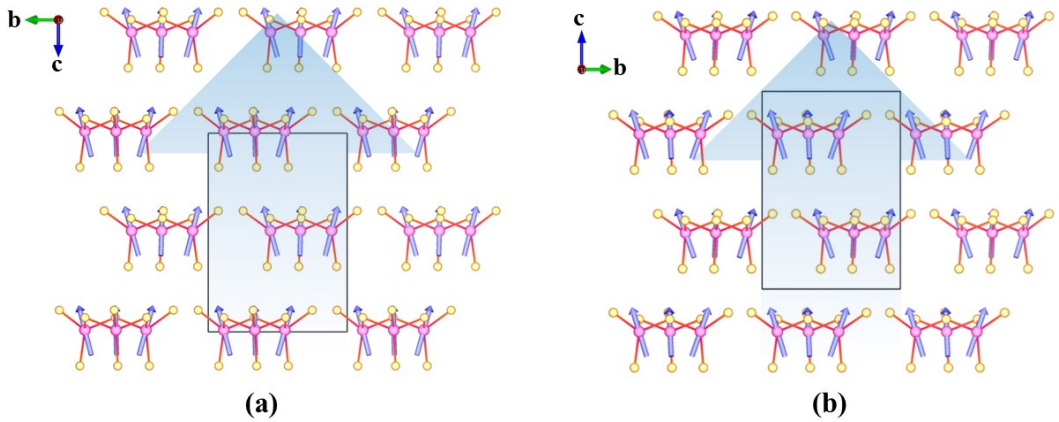

Fig. S7 The polarization direction (the purple arrow directions) of the $[Ge_3S_9]$ rings in $[NaSr_4Cl][Ge_3S_{10}]$ (a), and $[Sr_4Cl_2][Ge_3S_9]$ (b).

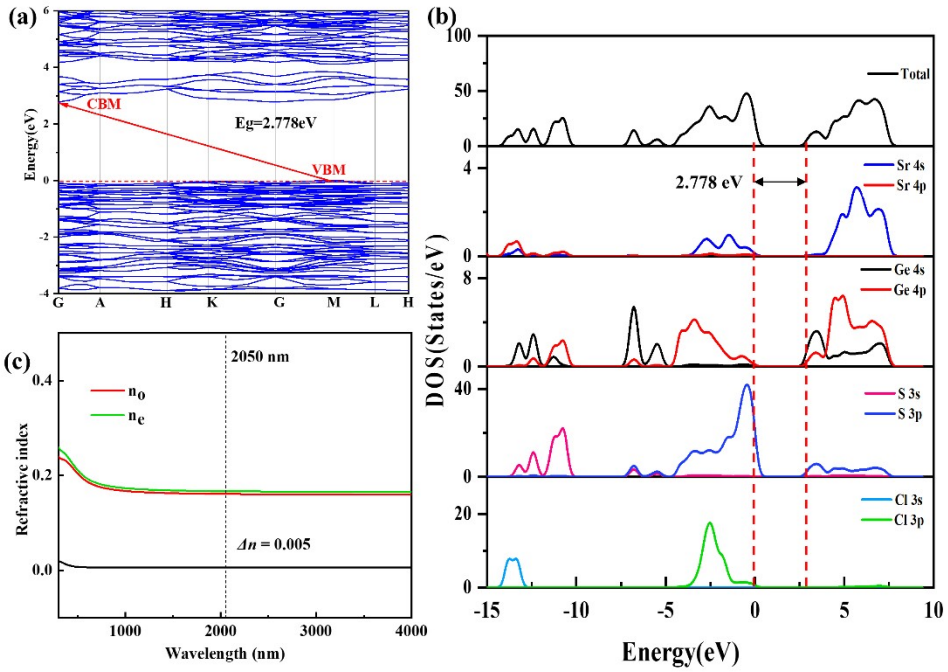

Fig. S8 The calculated bandgap (a), the projected density of states (b), and the calculated birefringence (Δn) curves of $[Sr_4Cl_2][Ge_3S_9]$ (c).

References

1. H. Yu, W. Zhang, J. Young, J. M. Rondinelli and P. S. Halasyamani, Bidenticity-Enhanced Second Harmonic Generation from Pb Chelation in $Pb_3Mg_3TeP_2O_{14}$, *J. Am. Chem. Soc.*, 2016, **138**, 88-91.
2. G. M. Sheldrick, SHELXT– Integrated space‐group and crystal‐structure determination, *Acta Crystallogr.*, 2015, **71**, 3-8.
3. G. M. Sheldrick and G. M. Sheldrick, *Acta Crystallogr., Sect. A: Found. Crystallogr.,* 2008, **64**, 112.
4. A. Spek, Single-crystal structure validation with the program PLATON, *J. Appl. Crystallogr.,* 2003, **36**, 7-13.
5. J. Tauc, Absorption edge and internal electric fields in amorphous semiconductors, *Mater. Res. Bull.*, 1970, **5**, 721-729.
6. S. Kurtz and T. Perry, A powder technique for the evaluation of nonlinear optical materials, *J. Appl. Phys.,* 1968, **39**, 3798–3813.
7. S. J. Clark, M. D. Segall, C. J. Pickard, P. J. Hasnip, M. I. Probert, K. Refson and M. C. Payne, First principles methods using CASTEP, *Z. Kristallogr. – Cryst. Mater.,* 2005, **220**, 567–570.
8. J. P. Perdew, K. Burke and M. Ernzerhof, Generalized gradient approximation made simple, *Phys. Rev. lett.*, 1996, **77**, 3865.
9. J. P. Perdew, J. A. Chevary, S. H. Vosko, K. A. Jackson, M. R. Pederson, D. J. Singh and C. Fiolhais, Atoms, molecules, solids, and surfaces: Applications of the generalized gradient approximation for exchange and correlation, *Phys. Rev. B*, 1992, **46**, 6671.
10. H. J. Monkhorst and J. D. Pack, Special points for Brillouin-zone integrations, *Phys. Rev. B*, 1976, **13**, 5188.